International Journal of Engineering Trends and Technology
ISSN: 2231 – 5381 /doi:10.14445/22315381/IJETT-V69I10P203
Volume 69 Issue 10, 15-19, October, 2021

Low power And Cost-Optimized Equipment Design For The Measurement of Resistivity In Austenitic Steels

Edgar Apaza Huallpa[1], Lino ReynaldoQuispe Cardenas[2], Alejandro Boris Marquez Guevara[3], Erick Omar Tunqui Labra[4]

[1,2,3,4]*Universidad Nacional de San Agustin de Arequipa, Perú*

[1]eapazahu@unsa.edu.pe, [2]lquispecarde@unsa.edu.pe, [3]amarquezg@unsa.edu.pe

Abstract *— This work presents an optimized, low-cost interface to detect strain-induced martensite in austenitic steels using the four-point resistivity measurement model, employing the ATmega328P microcontroller and other carefully selected components. It was designed as a system with several subunits implemented as modules to greatly aid troubleshooting in case of system failure. It is suitable for testing low impedance metals, such as austenitic, ferritic, and martensitic steels. It ensures internet connectivity for better display and data processing, as well as current optimization, thus reducing overall power consumption, which makes the device ideal for use in off-grid environments. This meter injects currents from 0.1A to 1.5A. Its ability to accept analog input and display digital output gives it the advantage of minimizing system errors associated with data display and processing. The meter was tested through simulations performed in Proteus, Simulink, Matlab, Thingspeak, among others, according to the design characteristics, so the data generated were compared with the input values, which shows the good resolution and repeatability of the equipment.*

Keywords *— electrical resistivity meter, digital, microcontroller, current injection, amplifier.*

I. INTRODUCTION

Currently, the use of austenitic steels is extended to several industrial fields due to their good mechanical strength and anti-corrosive properties [1]; one of the main ones is the cold forming industry which involves several phenomena that can be studied by the measurement of resistivity [2].

Hardening in austenitic steels by a mechanical process is usually the result of plastic deformation of the lines near the surface. Cold working causes microstructural changes of the material due to deformation, formation of new grains, and increase of defect density [3]. The method used for characterizing this phenomenon is the four-point resistivity measurement, initially proposed by F. Werner [4], which is generally used for metallic and semiconductor materials.

This work considers the mathematical theory in the measurement of resistivity and the use of electronic components for developing equipment that works with a portable power source. This allows its easy use and manipulation in fieldwork, the sections of such as the shaping of steels and welded joints, which are usually difficult to access.

II. THEORETICAL PRINCIPLE OF RESISTIVITY MEASUREMENT

The four-point method is developed under the following points. a) It is considered for the current reading process (i) the external tips and for the voltage reading (V) the internal tips as well as the distance between the four tips are equal b) The tips of the probes should be placed as close as possible to the center of the specimen with a maximum error of 10% [5]. For calculating the resistivity in plates of defined width, length, and thickness, equation (1) is used.

$$\rho = 2\pi s \frac{V}{i} F_1 F_2 \tag{1}$$

Where s is the distance between the probe tips, F_1andF_2shape correction factors are calculated from equations (2)and (3), respectively.

$$F_1 = 1 + 4\frac{s}{w}\left[\sum_{n=1}^{\infty}(-1)^n\left(\frac{1}{\sqrt{\left(\frac{s}{w}\right)^2 + (2n)^2)}} - \frac{1}{\sqrt{\left(2\frac{s}{w}\right)^2 + (2n)^2)}}\right)\right] \tag{2}$$

Where s represents the distances between the contacts and w the thickness of the specimen, which is tabulated in table (1) below.

Table 1. Tabulated values for F_1

w/s	Correction factor F_1
0,1	528652,992
0,2	292,4402
0,3	26,4022
0,4	8,3738
0,5	4,3669
0,6	2,9094
0,7	2,2225
0,8	1,8444
0,9	1,6141
1,0	1,4635

$$F_2 = \frac{\pi}{\left\{\left(\pi\frac{s}{d}\right) + \ln\left(1 - e^{\frac{-4\pi s}{d}}\right) - \ln\left(1 - e^{\frac{-2\pi s}{d}}\right) + \left[e^{-2\pi\left(\frac{a}{s}-2\right)\frac{s}{d}}\left(\frac{\left(1-e^{\frac{-6\pi s}{d}}\right)\left(1-e^{\frac{-2\pi s}{d}}\right)}{\left(1+e^{\frac{-2\pi s}{d}}\right)}\right)\right]\right\}} \quad (3)$$

Where d expresses the length of the specimen and a the width which are tabulated in the table (2).

Tabla2. Tabulated values for F_2

$\frac{d}{s}$	$\frac{d}{s}=1$	$\frac{d}{s}=2$	$\frac{d}{s}=3$	$\frac{d}{s}\geq 4$
1,0			0.9988	0.9994
1.25			1.2467	1.2248
1.5		1.4788	1.4893	1.4893
1.75		1.7196	1.7238	1.7238
2.0		1.9454	1.9475	1.9475
2.5		2.3532	2.3541	2.3541
3.0	2.4575	2.7000	2.7005	2.7005
4.0	3.1137	3.2246	3.2248	3.2248
5.0	3.5098	3.5749	3.5750	3.5750
7.5	4.0095	4.0361	4.0362	4.0362
10.0	4.2209	4.2357	4.2357	4.2357
15.0	4.3882	4.3947	4.3947	4.3947
20.0	4.4516	4.4553	4.4553	4.4553
40.0	4.5121	4.5129	4.5129	4.5129
∞	4.5324	4.5324	4.5325	4.5324

III. DESCRIPTION OF PROPOSED SYSTEM

The model shown in Fig. 1 employs the four-point test proposed by L.B. Valdes [6] by allocating a current through the specimen and measuring the voltage drop across the specimen [7]. The ATmega328P microcontroller is used to select the current supplied through the keyboard-LCD interface, and the latter will be the means to enter the dimensions of the specimen, as well as to record and send the data to the Thingspeak platform for the subsequent analysis of the martensite generated after the test.

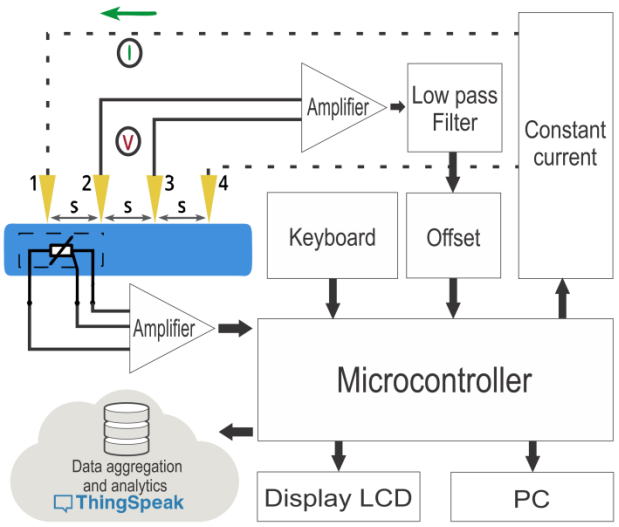

Fig. 1: Block diagram

A. *Circuit design*

The circuit was developed using the Proteus software (Fig. 2), which has been divided into stages, including the signal conditioning comprising a buffer amplifier, an instrumentation amplifier, and an offset stage that is coupled to an analog input of the microcontroller; it also has a constant current module, the interface for communication with the device and the power supply module adapted to a 1 cell LiPo battery.

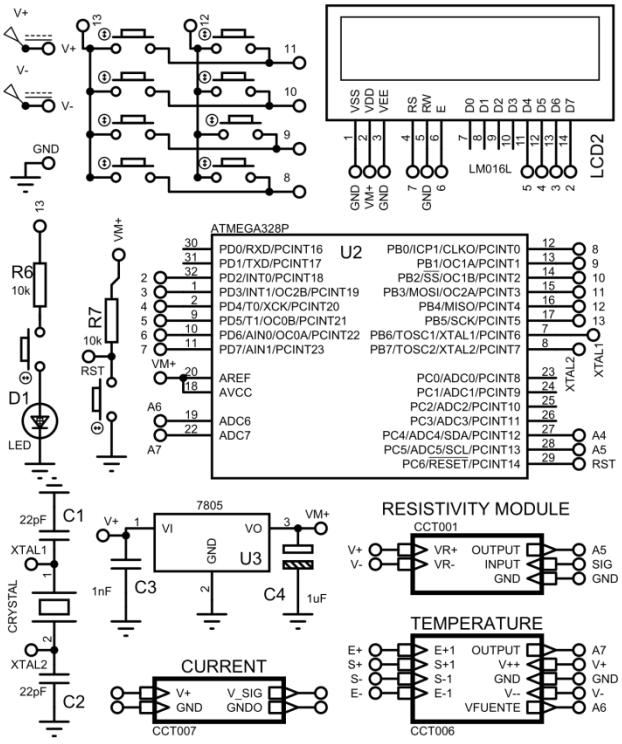

Fig. 2: Proposed circuit made in Proteus

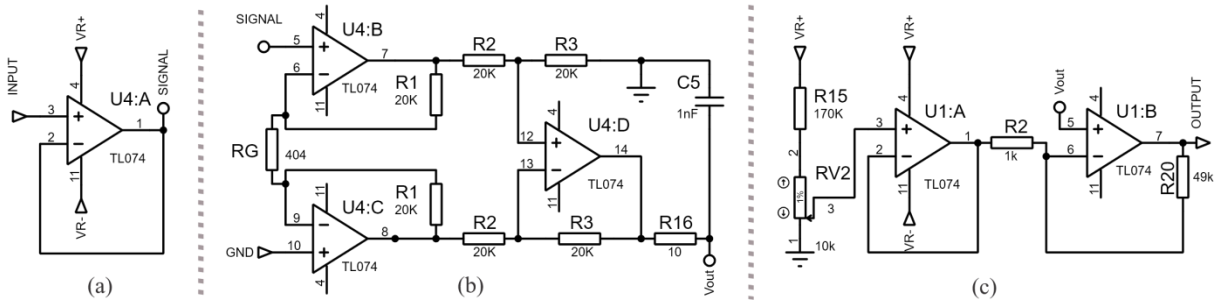

Fig. 3: (a) Buffer amplifier (b) Instrumentation amplifier (c) Offset adjustment

a) Signal conditioning: The buffer amplifier is shown in Fig.3a. Consists of an OpAmp and is responsible for matching the low impedance of the probe to the instrumentation amplifier.A three Op-Amps – based INA architecture [14], [15], [16], [17], [18] as shown in Fig.3b. It consists of two non-inverting amplifiers at the input side of the INA, and a difference amplifier, also known as a subtractor, forms the output stage of INA. The gain of this INA configuration is specified using the feedback resistors R1, RG, R2, and R3. The matching of the resistors together with their large value is the key to the high CMRR of this INA architecture [19]. This configuration amplifies the voltage drop by 100. Its behavior is described in expression (4). Where $V_1, V_2$are the input voltages to the first two amplifiers,$R_1$is part of the internal gain setting resistors, $R_g$the gain resistance and finally the output voltage,V_{out} [8].

$$Gain = \frac{V_{out}}{V_1 - V_2} = 1 + \frac{2 * R1}{RG} = 100 \qquad (4)$$

The buffer type OpAmp and the one used in the instrumentation configuration is the TL074 as it has low noise and high common-mode rejection characteristics. The signal from the instrumentation amplifier goes through a passive RC filter that has the function of eliminating high-frequency signals caused by electrical noise. Equation (5) [9] was used for the calculation.

$$F_c = \frac{1}{2\pi R * C} \qquad (5)$$

b) Offset adjustment: Its objective is to take full advantage of the ADC combinations of the microcontroller. This sub-stage has two Opamps, one of which is of the buffer type, and the other has a non-inverting configuration which can be seen in Fig. 3c. The first configuration has the purpose of adapting the impedance of a potentiometer that provides an offset voltage to the inverting input of the Opamp. The second one has the purpose of amplifying by 50 the output value of the instrumentation amplifier. The following equation (6) describes the joint dynamics of the above-mentioned configurations. Where $V_{out}$is the output voltage, $V_{in}$is the input voltage, $G$is the gain and$V_{of}$is the offset voltage.

$$V_{out} = V_{in}(G + 1) - V_{of}G \qquad (6)$$

c) Constant current module: It is comprised of an electronic load system, the characteristic of which is maintaining the current at an assigned level [10]. This is set based on the value displayed on the LCD display and a multi-turn potentiometer assigned for this purpose. Due to the feedback is given to the Opamp the current remains fixed at the set value, even if the source working in the power stage has disturbances. Given the configuration of the mosfet, it has to dissipate energy in the form of heat, making it essential to use a heat sink proportional to its size.

d) Temperature module: It consists of a Wheatstone bridge and an instrumentation amplifier circuit that allows obtaining the voltage variation depending on the temperature in the specimen. This equipment has the purpose of applying a correction value according to the temperature increase that occurs in the specimen.

e) Power supply module: The power supply module consists of the 3.7v LiPo battery, its charger module, as well as two compact Boost type voltage boosters, which maintain a voltage of 5.5v at its output for the power supply of the microcontroller, OpAmps, and other elements of the circuit. This set allows ensuring the portability of the equipment.

f) Communication module: The communication between the user and the device is given by a keyboard with a configuration specially designed for the application and an LCD display. The ESP8266-01 WiFi module is used to display the data and to connect to the internet, which has the appropriate dimensions and other characteristics for use in the equipment.

B. Data acquisition

Data acquisition is provided by the ATmega328P microcontroller, which has a 10-bit ADC and a working voltage of 5 volts. The output of the operational amplifier thus has to conform to this characteristic.

C. Program description

The program shown in Fig. 4 starts by displaying a welcome message. Firstly, the menu is displayed where the value of the area (mm^2) of the specimen to be tested must be entered. Secondly, the length [11] of the specimen must be entered, and the third menu is then displayed indicating the current level to be used for the test [12]; the potentiometer must be turned until the optimum current level is reached. Once the values have been entered, you will be asked how to visualize the data. In this option, the operator must choose according to the situation; in case of pressing the A key, the values will be automatically visualized on the LCD display. If the B key is pressed, the data will be visualized and acquired by the computer through the serial communication cable.

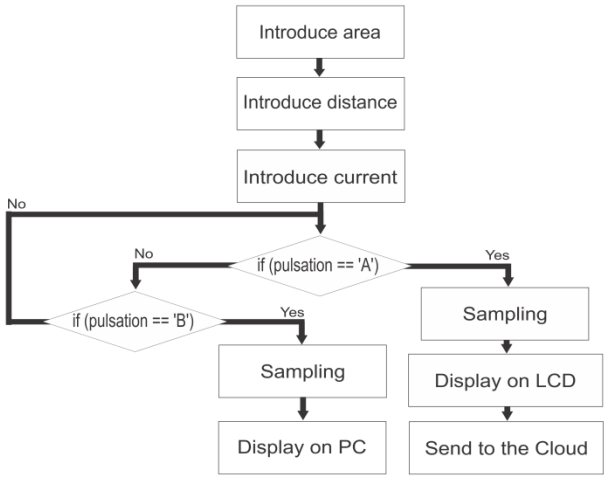

Fig. 4: Algorithm used to manipulate the equipment

IV. SIMULATION OF THE CIRCUIT OPERATION

A. Accuracy

By means of ammeters and voltmeters at the input and output of the circuit simulated in Proteus, it was possible to verify that the gain had errors equal to or less than 13.76% (due to the bypass voltage and the resolution of the potentiometers) with a resistance of 160uΩ and currents within a step of 0.5A. For this simulation, a supply voltage to the amplifiers of ±5.3V and an offset value of 0V were used.

Table 3: Comparative values

Input voltage	Input current	Output voltage	Gain	Error
80uV	0.5A	0.455V	5688	13.76%
160uV	1.0A	0.855V	5344	6.88%
240uV	1.5A	1.250V	5208	4.16%

The next step was to place a variable current using a current curve approximating the one proposed by [13] where the accuracy with which each point follows the signal conditioning stage to the input value is verified, using a virtual terminal (Fig. 5a), Simulink and Matlab, since Proteus does not have data storage.

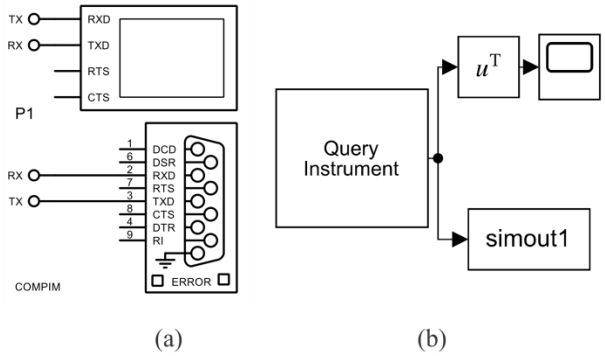

Fig. 5: Additional components. (a)Communication in Proteus, (b) Diagram in Simulink.

To the circuit shown in Fig.3, it was necessary to add a monitor and a virtual communication bus (Fig. 5b), and for data reception, it was necessary to use the Query instrument, Math operation, for the workspace and scope blocks. This tool made it possible to visualize the data over time and compare them with the values set at the beginning, reflecting a small margin of error, as shown in Fig 6.

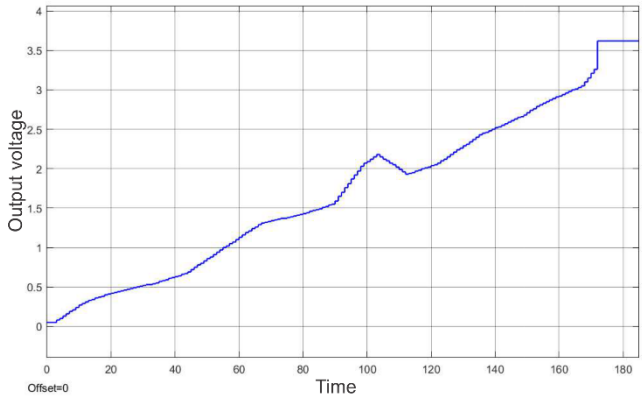

Fig.6: Voltage vs. time graph in Simulink

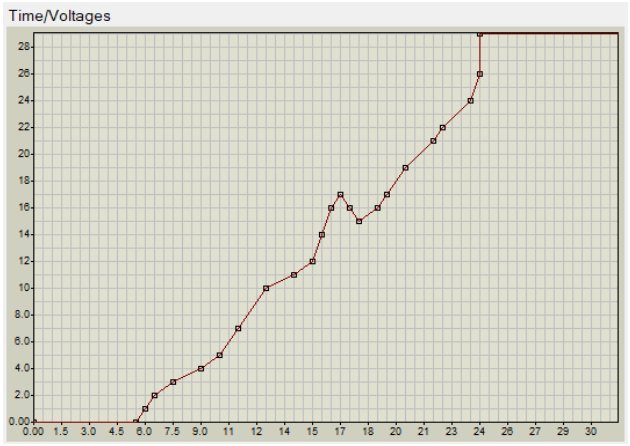

Fig. 7. Input Voltage in Proteus

The behavior of the input voltage of the amplifier shown in Fig. 7 increases progressively from 0V to 29V, which is reflected in the resistance used, in the range from 0V to 725uV. A similar graph of the output voltage that was recorded on the serial monitor and LCD accompanying the microcontroller can be seen.

B. Sending data

To send the data to the Thingspeak platform, it was necessary to configure the TX and RX communication output of the microcontroller as a data frame, which was sent through a serial port to establish communication with the Thingspeak API Key. A phyton program is needed in order to generate a link between proteus and the API Key used. The communication in Proteus occurs through the virtual port generated by the COMPIM, and the frame of values sent by the serial monitor can be seen in Fig. 8.

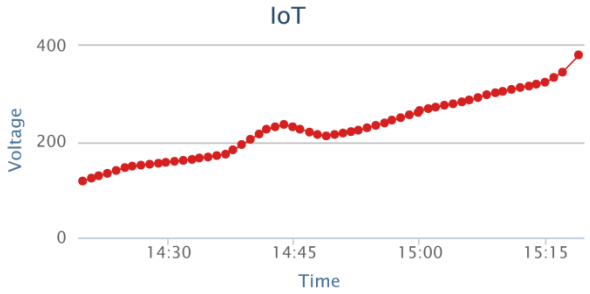

Fig. 8: Voltage vs. time data on the Thingspeak Platform

The simulation shows the voltage variation over time, highlighting the ability to replicate data from the source.

VI. CONCLUSIONS

The article gives a description of the operation of the equipment in a simulated environment demonstrating the following points: a) The feasibility of a new design for measuring resistivity based on the ATMEGA 328P microcontroller with acceptable accuracy. b) The usefulness of the equipment for characterizing the mechanical properties of conductive materials. c) The simulation showed that the equipment is capable of measuring and recording resistivity data in real-time. d) The tracking and repeatability of the measurements performed in simulation are verified taking into consideration the real characteristics of each component.The components selected will be placed on a PCB, which will be developed on the easyEDA platform to provide a compact piece of equipment for testing.

The design of the proposed equipment provides the basis for a future development that will allow evaluating and characterizing the mechanical properties of austenitic steels by measuring their resistivity, in addition to the study of martensitic transformation by deformation in a continuous way in a tensile test.

ACKNOWLEDGMENT

This work was funded byUniversidad Nacional de San Agustin de Arequipa, UNSA(N° Contrato IBA-IB-26-2020-UNSA).

REFERENCES

[1] LoK. H., ShekC. H. and Lai J. K. L., Recent developments in stainless steels Mater. Sci. Eng. R 65 (2009) 39–104.

[2] Mayer, Patrick, Kirsch, Benjamin, Müller, Christopher, Hotz, Hendrik, Müller, Ralf, Becker, Steven, et al. Deformation induced hardening when cryogenic turning. In CIRP Journal of Manufacturing Science and Technology 23 (2018) 6–19.

[3] Jawahir, I.S., Brinksmeier, E., M'Saoubi, R., Aspinwall, D.K., Outeiro, J.C., Meyer, D., et al. Surface integrity in material removal processes: recent advances. CIRPAnnals 60 (2) (2011) 603–626.

[4] Wenner, F., Bulletin of the Bureau of Standards. (1915) 12, 469.

[5] Emerson M. Girotto, Ivair A. Santos,Medidas de resistividade elétrica dc em sólidos: como efetuá-las corretamente. Quim. Nova. 25(4) (2002) 639-647.

[6] Valdes, L.; Proc. I.R.E. (1954) 42, 420.

[7] Lu, Y., Santino, L. M., Acharya, S., Anandarajah, H., D'Arcy, J. M.Studying electrical conductivity using a 3D printed four-point probestation.(2017).

[8] Savant, C. J., Roden, M. S., Carpenter, G. L., Cázares, G. N.,Diseñoelectronico: circuitos y sistemas, Addison-Wesley Iberoamericana. (1992).

[9] Mikailu, A., Abdullahi, I., Sani, M. G., Muhammad, S.,Developmentof Digital Resistivity Meter, Advances in Physics Theories and Appli-cations.(2015).

[10] Igboama, W. N., Ugwu, N. U.Fabrication of resistivity meter and itsevaluation, American Journal of Scientific and Industrial Research. (2011) 713-717.

[11] Rougerio T. da Rocha, R. T., Gutz, I. G., Do Lago, C. L., A low-cost and highperformance conductivity meter, Journal Chemical Education. 74(5) (1997) 572.

[12] Yohandri, Y., Mairizwan, M., Akmam, A., Development of aDigital Resistivity Meter Based on Microcontroller. (2018).

[13] Hidefumi Date,MasatnshiFutakawa, ShuichIisihilr, Strain Rate on Electric Resistivity of Austenitic Stainless Steel, JSME/ASME International Conference in Materials and Procesing. (2002) 48-51.

[14] M.A. Smither, D.R. Pugh, L.M. Woolard,C.M.R.R. analysis of the 3-op-amp instrumentation amplifier,IEEE Journals & Magazines, Electronics Letters. 13(20) (1977).

[15] H. Chow and J. Wang,High CMRR instrumentation amplifier for biomedical applications,2007 9th International Symposium on Signal Processing and Its Applications. (2007) 1-4.

[16] A. Harb and M. Sawan,New low-power low-voltage high-CMRR CMOS instrumentation amplifier,1999 IEEE International Symposium on Circuits and Systems (ISCAS). 6(1999) 97-100.

[17] M. Goswami and S. Khanna,DC suppressed high gain active CMOS instrumentation amplifier for biomedical application,2011 International Conference on Emerging Trends in Electrical and Computer Technology. (2011) 747-751.

[18] Chih-Jen Yen, Wen-Yaw Chung and Mely Chen Chi,MicroPower Low Offset Instrumentation Amplifier IC Design For BioMedical System Applications, IEEE Transactions On Circuits And Systems:Regular Papers. 51(4) (2004) 691-699.

[19] M. Konar, R. Sahu and S. Kundu,Improvement of the Gain Accuracy of the Instrumentation Amplifier Using a Very High Gain Operational Amplifier,2019 Devices for Integrated Circuit (DevIC).(2019) 408-412.